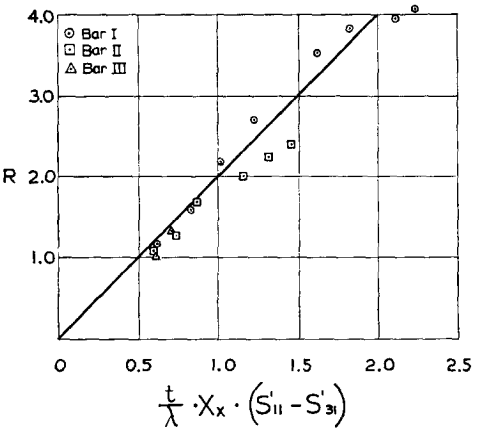

FIG. 3. Retardation for various loads for all three silicon bars. Retardation below one λ could not be determined.

in Fig. 1. Their central sections were illuminated by infrared light polarized in the vertical plane. The light transmitted through the silicon continued through a Polaroid infrared crossed polarizer in the horizontal plane and the image was viewed by an RCA 6032A image converter tube. The wavelength was held at 1.2 μ, the minimum observable through silicon and the maximum converted by the image tube.

Figure 2 was taken of bar I when subjected to a stress of 10.0×10^8 dynes/cm^2 in its outer fiber. The fringes correspond to a retardation of 3.8 wavelengths (from the neutral plane in the center of the bar to its edge). The apparent curvature of the bar is due to distortion by the image tube.

In pure bending there is only one stress, the longitudinal one, X_x, and the relation can be expressed as

$$R=c\cdot t\cdot X_x\cdot(S_{11}'-S_{31}')/\lambda,$$

where S_{11}' is the elastic compliance constant along the x axis and S_{31}' along the z axis.

Figure 3 is a plot of R *vs* $t\cdot X_x\cdot(S_{11}'-S_{31}')/\lambda$ for various loads on the three silicon bars. It indicates the variation in the results and gives a strain optical value of 2.0. The elastic compliance constants were calculated from the elastic stiffness constants for silicon given by Conwell,[4] and are given in Table I.

The strain-optic value of 2.0 obtained here compared favorably with the two values quoted by R. Bullough.[5] These were 1.0 from P. D. Fochs and 2.3 from W. L. Bond.

While the light transmitting surfaces of these bars were optically polished, it was later found that a 1-1-1 polish etch of hydrofluoric, nitric, and acetic acids produces a surface that transmits infrared light satisfactorily. This markedly reduces the time necessary for specimen preparation.

[1] W. C. Dash, Phys. Rev. **98**, 1536(A) (1955).
[2] P. Penning, Philips Research Repts. **13**, 96 (1958).
[3] M. M. Frocht, *Photoelasticity* (John Wiley and Sons, Inc., New York, 1941), Vol. I, p. 136.
[4] E. M. Conwell, Proc. Inst. Radio Engrs. **40**, 1327 (1952).
[5] R. Bullough, Phys. Rev. **110**, 620 (1958).

Modifications of the Lomnitz-Jeffreys' Law of Creep

J. ROSS MACDONALD
Texas Instruments Incorporated, 6000 Lemmon Avenue, Dallas 9, Texas
(Received December 11, 1958)

A CONSIDERABLE number of creep functions, $\phi(t)$, have been proposed to represent experimental creep data in solids. Some of them, such as Lomnitz's function[1,2] $\phi(t)=q\ln(1+t/\tau_0)$, where q and τ_0 are constants, suffer from the difficulty that they predict infinite final strain for constant applied stress. Others, such as the power law,[2,3] have the defect that they lead to an infinite initial rate of creep as well.

For small strains in many materials, it should be an excellent approximation to consider linear behavior only. For a linear system, it can readily be shown that only finite final strain can occur. This condition is met when the integral over-all relaxation times (discontinuous or continuous) of the system is finite.[4] An infinite value for this integral, which indicates that the distribution-of-relaxation-times function for the system is non-normalizable, means that the system must have an infinite number of concentration of relaxation times. For a linear material of finite size having a finite number of atoms, such an infinite value is impossible.

Lomnitz found that his $\phi(t)$ function could explain a considerable amount of experimental creep data well.[1] In addition, it led to $1/Q$ substantially constant over a wide frequency range, again in agreement with much experimental data.[2] Here Q is a quality factor representing the ratio of energy per cycle stored in the system to that dissipated for sinusoidal excitation. Recently Jeffreys[5] has shown that a simple generalization of Lomnitz's function explains even further data. Jeffreys' result is

$$\phi(t)=(q/\nu)[(1+t/\tau_0)^\nu-1],$$

a generalization as well of the power law. Here ν is a constant lying in the range $0\leqslant\nu<1$, and Lomnitz's result is obtained for $\nu\to0$. The corresponding rate-of-creep function is $A(t)=d\phi/dt=(q/\tau_0)\cdot(1+t/\tau_0)^{\nu-1}$. Although this creep function leads to a finite initial rate of creep, it still predicts an infinite final strain and thus represents a physically unrealizable linear system.

When the distribution of relaxation times function for the above $A(t)$ is obtained by means of an integral transform,[4] it is found that it is non-normalizable because the density of relaxation times falls off too slowly for very long relaxation times. Since the Lomnitz-Jeffreys' (abbreviated hereafter as L-J) function may be expected to explain a wide variety of experimental data well, it is of interest to show how it may be modified so that the resulting function represents a physically realizable linear system yet the essentials of the response of the system remain unaltered in regions where the original function shows good agreement with experiment. There are a number of ways to make such a modification. Two possible new rate of creep functions are,

$$A(t)=(q/\tau_0)[(1+t/\tau_0)^{1-\nu}+(t/\tau_\infty)^2]^{-1}$$

or $(q/\tau_0)[\exp(-t/\tau_\infty)][1+(t/\tau_0)]^{\nu-1}$. When $a\equiv\tau_0/\tau_\infty$ is much smaller than unity, these functions will show L-J response for long times and to very low frequencies. By taking τ_∞ sufficiently large, the range of agreement can be extended indefinitely. The final strain will still be finite, however, and, as Jeffreys points out,[5] mountains and buildings will therefore stand.

There is a further way to achieve physical realizability. The distribution of relaxation times function corresponding to the L-J $A(t)$ is $G(\tau)=(q/\tau_0)(\tau/\tau_0)^{\nu-1}[\exp(-\tau_0/\tau)]/\Gamma(1-\nu)$. Physical realizability may be ensured by arbitrarily setting $G(\tau)=0$ for $\tau\geqslant\tau_\infty$. A slightly better approximation is to make a discontinuous change in slope of $G(\tau)$ for $\tau>\tau_\infty$ while keeping $G(\tau)$ itself continuous at this point. A final slope of -2 instead of the original $-(1-\nu)$ will make normalization of $G(\tau)$ possible and lead to convergent values of all other integrals associated with it.

The $1/Q$ factor for the Lomnitz-Jeffreys' function can be expressed in terms of Lommel functions of a single variable.[6] Since these functions are very poorly tabulated, $1/Q$ must be calculated (as a function of frequency) by means of mechanical quadratures. Such a mode of calculation is also required for the various modified functions proposed herein, and work is in progress on obtaining the plane wave response of systems described by some of these modified functions using a digital computer.[7]

The $\phi(t)$ and $A(t)$ functions may be obtained explicitly for the exponentially modified L-J functions and for the modified distribution-of-relaxation-times approach. For the latter with

constant final slope, one finds, for example,

$$A(t)=\frac{q}{\tau_0\Gamma(1-\nu)}\left[\frac{\Gamma(1-\nu,\, a+t/\tau_\infty)}{(1+t/\tau_0)^{1-\nu}}+a^{1-\nu}e^{-a}\left(\frac{\tau_\infty}{t}\right)^2\left\{1-(1+t/\tau_\infty)e^{-t/\tau_\infty}\right\}\right],$$

which approximates well to the original $A(t)$ for $t\ll\tau_\infty$. Note that $A(0)$ is finite and $A(\infty)=0$. The corresponding $\phi(\infty)$ function reduces for $a\ll 1$ to

$$\phi(\infty)\cong\begin{cases}qa^{-\nu}(1+\nu^{-1})/\Gamma(1-\nu) & 0<\nu<1\\ q(1-\ln a) & \nu=0\end{cases}.$$

When $G(\tau)$ is taken zero for $\tau>\tau_\infty$ the unity terms in $(1+\nu^{-1})$ and $(1-\ln a)$ disappear. The exponential modification leads to a rather unlikely distribution of relaxation times but to very similar $\phi(\infty)$ results for a $\ll 1$. For $0<\nu\leqslant 1$, one finds $\phi(\infty)\cong qa^{-\nu}\Gamma(\nu)$, and for $\nu=0$, $\phi(\infty)\cong -q\ln a$.

The author is much indebted to Dr. C. Lomnitz for drawing his attention to the present problem.

[1] C. Lomnitz, J. Geol. **64**, 473 (1956).
[2] C. Lomnitz, J. Appl. Phys. **28**, 201 (1957).
[3] B. Gross, J. Appl. Phys. **18**, 212 (1947).
[4] J. R. Macdonald and M. K. Brachman, Revs. Modern Phys. **28**, 393 (1956).
[5] H. Jeffreys, Geophys. J. **1**, 92 (1958).
[6] G. N. Watson, *Theory of Bessel Functions* (Cambridge University Press, London, 1944), second edition, pp. 345–352.
[7] C. Lomnitz and J. R. Macdonald (paper in preparation).

Correlation between Mobility and Effective Mass in Semiconductors

ROBERT W. KEYES
Westinghouse Research Laboratories, Pittsburgh 35, Pennsylvania
(Received August 27, 1958)

THEORIES of the scattering of electrons in semiconductors by interaction with the lattice vibrations show that the electron mobility is rather strongly dependent on the effective mass.[1] For example, the expression for the mobility which is obtained from the simple deformation potential theory for a spherical energy band contains the effective mass to the minus $\frac{5}{2}$ power as a factor.[2] The use of these theories to correlate effective mass with mobility among different semiconducting materials is not straightforward, however, as the strength of the lattice-electron coupling and the types of lattice modes involved in the scattering vary from material to material. Nevertheless, in this note we will compare the mobilities and effective masses of various current-carrying entities in several semiconductors and point out the existence of a relationship between the effective mass measured by cyclotron resonance experiments[3] and the lattice mobility at 300°K.

The relationship is illustrated in Fig. 1, in which μ_L, the lattice scattering mobility at 300°K, is plotted against m^*, the effective mass, for all of the current carriers in semiconductors for which the values of the parameters have been fairly well established. In the anisotropic cases, a reciprocally averaged inertial mass has been used for m^*. In cases in which deviations from a quadratic dependence of energy or crystal momentum are important, an attempt has been made to use the effective mass at the bottom of the band.

Figure 1 shows that μ_L varies approximately as $m^{*-1.35}$. The dotted line in Fig. 1 shows that $\mu_L\sim m^{*-1}$ gives a somewhat rougher representation of the data. This representation is of interest, however, because the mobility can be related to a relaxation time by the equation $\mu_L=e\tau_L/m^*$ and the dotted line is a line of constant τ_L. Thus, it is seen that, even though, for the carriers considered, the mobility varies over two orders of magnitude, τ_L varies only through a factor four.

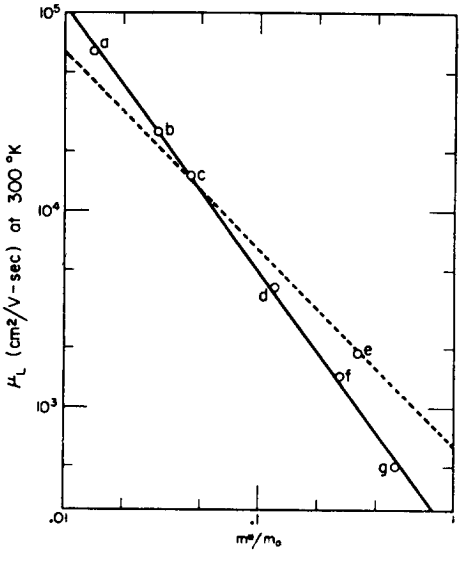

FIG. 1. A plot of lattice mobility at 300°K *vs* effective mass for a number of current carriers in semiconductors. The identification of the carriers represented by the points is as follows: (a) electrons in InSb, (b) electrons in InAs, (c) light holes in Ge, (d) electrons in Ge, (e) heavy holes in Ge, (f) electrons in Si, (g) heavy holes in Si. The equation of the solid line is $\mu_L=210(m^*/m_0)^{-1.35}$ cm²/v-sec. The dotted line has slope -1, and corresponds to $\tau_L=3.6\times10^{-13}$ sec. The effective masses used are those obtained by cyclotron resonance or magneto-optic experiments. The mobilities are derived from a large number of sources. In some cases there are discrepancies between different authors, which, though significant for some purposes, do not appear large on the scale of this figure.

[1] For a recent review of mobility theory, see F. J. Blatt, in *Solid State Physics*, edited by F. Seitz and D. Turnbull (Academic Press, Inc., New York, 1957), Vol. 4.
[2] J. Bardeen and W. Shockley, Phys. Rev. **80**, 72 (1950).
[3] B. Lax, Revs. Modern Phys. **30**, 122 (1958).

Improvement in Floating Zone Technique

W. G. PFANN, K. E. BENSON, AND D. W. HAGELBARGER
Bell Telephone Laboratories, Inc., Murray Hill, New Jersey
(Received December 1, 1958)

THE round-rod, floating-zone technique[1–3] is limited to small diameters, because it is difficult to melt the entire cross section of a large diameter rod while keeping the zone height less than the maximum height supportable by surface tension. This height, as shown by Heywang,[4] is a constant at large radii and, at radii $<\sim 2(\gamma/\rho g)^{\frac{1}{2}}$, decreases with radius toward zero, where γ, ρ, and g denote surface tension, density, and the gravitational constant, respectively. The constant value, denoted l_m, is $2.8(\gamma/\rho g)^{\frac{1}{2}}$ for a particular shape of zone, which is about 0.7 cm for gold, tin, and water, and about 1.5 cm for silicon, titanium, and zirconium.

A way around the limitation on rod forms is to use forms of cross section small in thickness (to permit melting through without exceeding l_m) and large in width; that is, plates or pipes. Stable molten zones can be produced in such forms. In fact such *wide zones* can be as high as zones in large-diameter rods.

Three types of wide zones are shown in Fig. 1. Another useful type is a disk-shaped zone, which is really a special form of closed-end zone. Disk zone be established either in vertical or horizontal plates.

A disadvantage of open-end zones is that the ends, being curved in the horizontal plane, tend to pull inward. This effect can be counteracted, down to moderate plate thicknesses, by inclining the zone downward near the ends, so that the extra gravitational head opposes the inward pressure arising from surface tension. Closed-end zones are not subject to pull-in and have the further advantage that more than one zone at a time can be supported.